POTENTIALS OF LOAD CARRYING, STRUCTURAL INTEGRATED CONDUCTOR TRACKS

A. Pototzky[1], D. Stefaniak[1], C. Hühne[1]

[1]DLR- Institute of Composite Structures and Adaptive Systems
Email: alexander.pototzky@dlr.de

Keywords: structure integrated conductor tracks, FML, multifunctional structure

Summary

Within this paper a new approach to integrate conductor tracks directly into composite structures is presented. In contrast to conventionally integrated conductor tracks, the conductor tracks which are presented here are designed for load carrying purposes. For this purpose, a first evaluation of adapted conductor path geometry is manufactured. Subsequently, studies are carried out to determine which conditions must be given in order to insulate the conductor tracks from one another. Afterwards, the point at which the conductor tracks can be integrated will be considered. The paper ends with the demonstration of a structural component which has four structurally integrated conductor tracks.

Introduction

The increasing electrification of modern vehicles like more electrical aircrafts (MEA) requires a complex wiring harness, which is often accompanied by significant weight penalties. In order to decrease structural weight and reduce the cable installation time during assembly, the conductor paths were integrated directly into the structure. Instead of using conventional copper wires, metal foils are placed alternately between composite fiber laminates to build the whole structure.
An advantage of such an approach is that the electrical wires are part of the structural component and even have load carrying capacities. In order to be able to analyze and assess the potential of fiber reinforced composite with regard to structure-integrated conductor paths, mechanical tests and analytic calculation are performed.

The more electric aircraft

The power supply in conventional airplanes can be divided into four different systems which are supplied by the turbine (see Fig 1): The electrical system supplies the avionics systems, the position lights as well as the in-flight entertainment. The tasks of the pneumatic system ranges from maintaining cabin pressure, the supply of the air conditioning system to the ice protection system. All the actuators for controlling the aircraft are typically connected to the hydraulic system. The fuel and oil pumps are assigned to the mechanical network [1].

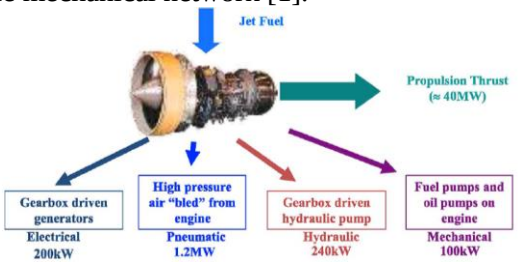

Figure 1: Power distribution of a conventional engine [1]

Figure 1 shows the four different performance systems with their corresponding performance requirements. The values provided refer to an aircraft of the size Airbus A320 or Boeing 737. The power demand which is required for such an aircraft ranges from 100kW for the mechanical systems up to 1.2MW for the pneumatic systems. It becomes clear that from 40MW total engine power 1.74MW for the different systems are branched off (4.35%)
The pneumatic system, which is designed as a bleed air system, causes the greatest power loss in the engine due to its architecture. By saving such a dosing system, the efficiency of the engine could be increased significantly [2].

All performance systems have evolved over the years. Studies show that the saving of individual subsystems lead to a significant increase in performance. In the course of the development of the "More Electrical Aircraft", the individual power systems will be gradually saved and replaced by an electrical system. With the launch of the B787, Boeing has taken a major step in this direction by completely dispensing with a pneumatic system [3].
The electrification of the aircraft also promises a significant reduction in the overall weight in addition to the cost savings in terms of maintenance and reduced fuel consumption [4].
Figure 2 shows the weight percentage breakdown for an aircraft with a seating capactity of 300. In consideration of an electrical aircraft, it is evident that the motors, generators and electrical cables dominate the electrical system weight.[5]

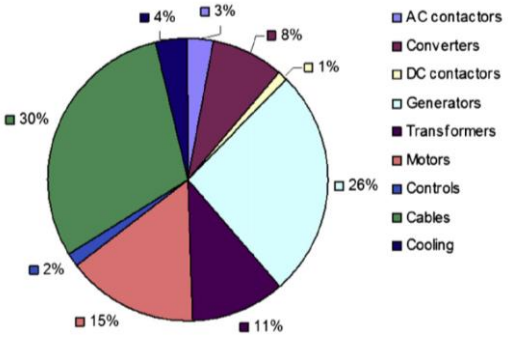

Figure 2: Percent of all electrical components in one aircraft [5]

There is a significant weight potential as there is about 30% of cable weight. Fortunately, the next generation aircrafts like the Airbus A350 and the Boeing B787 are made out of carbon-fiber-reinforced polymer (CFRP) as this Material is, as a consequence of its additive manufacturing, perfectly predestined to integrate the conductor path into the structure. Therby, it is possible to reduce more cable weight by substituting for example the insulating shell.

State of the art

Various attempts have already been made to integrate conductor tracks into a fiber composite component. Kim [6] examines copper cables that are integrated directly into the fiber composite structure. The copper strips were embedded in a glass fiber / epoxy material and tested with regard to fatigue. Under load, the conductor delaminated from the fiber composite and ruptured after 5500 cycles.
Another approach is to print the conductor tracks on the already cured component [7]. The conductor is unprotected on the surface and, depending on the geometry there are considerable changes in resistance under load.
Hufenbach shows in his investigations that both copper mesh as well as massive copper conductors reduce the residual strength of the samples [8]. Depending on the main fiber orientation, the influence is different.

Conductor geometry

In order to be able to transmit any electrical signal or power, a cable is used as reference. (cordless transmission systems are not considered at this point). A direct integration of these cables into the structure would show a disadvantageous behavior since the laminate`s smoothness is impaired by the cable. The conductor tracks must therefore be adapted to the structure. From the requirements of an electrical system, the minimum cross-section of a conductor is specified in normal case. Under this boundary condition, the shape of the conductor cross-section remains an arbitrary variable. In Figure 3 (top) the geometry change of different conductors with the same cross-section is shown. Different conductor heights are applied, which, with a constant cross-section, only dependend on the conductor width. The ratio of height to width of an elliptical cross-section is depicted in blue. A special case of this cross-section is the circular cross-section in which the ratio of width to height is exactly w/h = 1. This point is shown separately in the diagram on the curve. All electrical wires and cables conventionally used to transport information, have a circular cross-section. The height`s influence of a rectangular conductor on the laminate as a function of its width, shown in red. The special case with the aspect ratio w/h = 1, a square, is

also marked. In addition to these basic geometrical bodies, it is theoretically possible that an electrical conductor can assume any desired cross-section. This cross-section can be represented as a simple polygon. Each polygon (n-corner) with a real number of corners is located in the gray-marked area between the two red and blue colored curves. With an increasing number of corners, these polygons approach a circular or elliptical cross-section.

The graph shows that the influence of the conductor height on the laminate decreases continuously. According to Schmidt et al. the integration of electrical round conductors leads to a massive ondulation of the fibers. This leads to a massive delamination in the laminate under bending load conditions [9].

In Figure 3, the circumference of a circle and square conductor cross-section is shown at the bottom. The circumference or the surface area of the conductor increases with an increasing ratio of width to height. It becomes clear that, although the negative influence of the conductor on the fibers decreases with the change in the geometry (fiber constriction), the bonding surface increases to the same extent. A good connection between the conductor tracks and the CFK structure is absolutely necessary.

With a conductor height of 0.1 mm, the conductor tracks are approximately as high as a fiber layer.

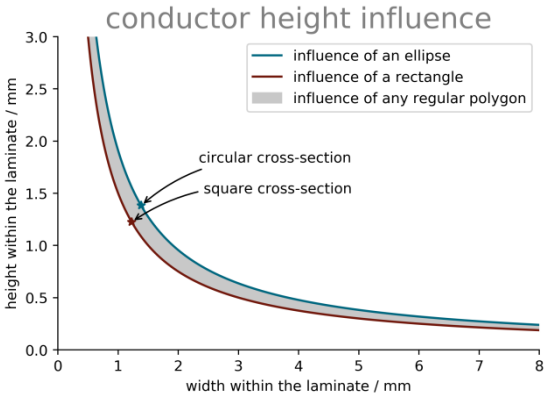

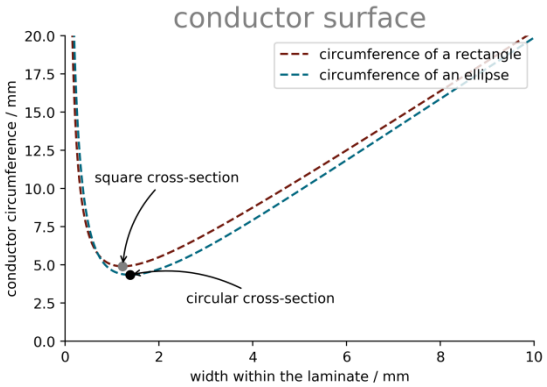

Figure 3: Conductors with a constant cross-section: As the width increases, the influence on the laminate (blue) decreases as the surface increases (red)

FML as conductive tracks

The last chapter shows, that it is useful to integrate conductor tracks that are as high as a single CFRP layer. Assuming that the conductor tracks are designed to be load-carrying, the selection of sensible materials is severely restricted.

Carbon fiber layers are electrically conductive. When electrically insulated from one another, they are able to conduct different voltages. In order to isolate the carbon fiber layers from each other, a glass fiber layer is suitable, since the glass fiber is electrically nonconductive. This results in a fiber composite structure which alternately has a certain number of carbon fiber layers and glass fiber layers. The number of carbon fiber layers therby determines the number of electrical signals or voltage potentials which can be transmitted via the structure. Compared to metallic conductors, however, carbon fiber is significantly higher-impedance [10], which leads to significant losses at high powers.

A completely different approach is the use of fiber metal laminates (FMLs). FMLs such as GLARE are well known and have been introduced to increase the material's damage tolerance [11]

Kolesnikov has proposed a local FML structure, consisting of several metal foils and a carbon fiber structure, in order to increase the joining strength in the connection area [12]. This has been extensively investigated, as shown in [13]. Furthermore, the mechanical

performance of Unidirectional CFRP has been improved by using metal layers as presented in [14].
An increased crash safety, especially under bending crash loading conditions, is also expected by several authors [15,16]
In addition to the already studied mechanical advantages, a further function is now to be added to the material: the electrically conductive layers are used to guide the electrical signals through the component. As already described, the mechanical properties of fiber composite structures and FMLs are adequately studied, so that the electrical properties are discussed in the following.
Two different types of samples are manufactured. One type is made from a GFRP / CFRP mix. The other sample type consists of two metal foils and a corresponding insulation made out of GFRP.

Electrical tests

When designing a component with integrated conductor tracks, it is necessary to determine the minimum spacing between the conductor tracks to prohibit any exchange of charge.
A charge exchange between two conductor tracks, which function as electrodes, leads to a voltage breakdown which occurs as a spark or as an arc. Such an arc destroys the insulation layer irreversibly because of its heat development. When designing the component, this scenario must be avoided in all circumstances. According to Grote et al. [17], the dielectric strength is equivalent to the electric field strength E. The field strength can be expressed by equation (1):

$$E = \frac{U}{d} \qquad (1)$$

(E= electrical field strength; U= voltage; d = distance of the conductor tracks)

In addition to the geometric distance between the electrodes (d) and the applied voltage (U), the dielectric between the conductor tracks plays a decisive role in the value of the dielectric strength.

Typically, the average breakdown strength of air is 3 kV / mm [17]. The breakdown strength of a fiber composite is strongly dependent on the fibers and the matrix. In this paper glasfiber reinforced plastics were investigated in detail. In contrast to carbon fiber, fiber glas rovings are electrically non-conductive. Nevertheless they are able to bear mechanical forces.
For identification of the breakdown voltage, samples were produced which consist of the two electrodes for applying the voltage and of different glass fiber layers to adjust the distance between the electrodes. Among one and five layers of glass fiber fabric were inserted between the electrodes. A layer of glass fiber (MTM44-1/GF0903-40%RW) has a nominal thickness of 0.101 mm, so that the breakdown strength can be derived by the number of layers. The electrodes were made out of carbon (MTM44-1/CF5804A-40%RW-DC) on the one hand, and on the other hand out of steel (X10CrNi18-8). Figure 4 shows the results of the investigation. Two results are displayed in this diagram, while the red bar is showing the breakdown strength for carbon fiber layers, the blue bar shows the dielectric strength of the specimen with integrated steel layers.

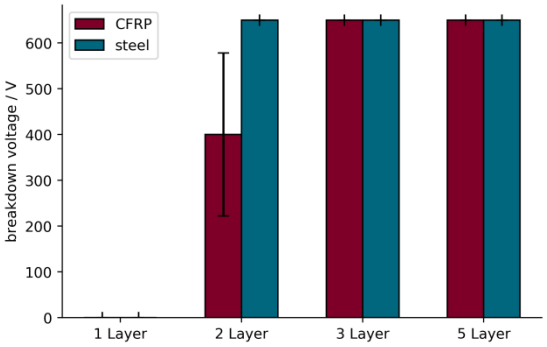

Figure 4: Breakdown voltage as a function of the glass fiber layers

It can clearly be seen that one layer of GFRP does not yet have an insulating effect. By adding another glass fiber layer, a voltage can be set between the two electrodes. The maximum voltage is 650 V for the steel conductor strips, which corresponds to the maximum allowed output of the power supply

unit. The mean dielectric strength of the three samples with the CFRP electrodes is 400V. The Samples vary in their dielectric strength between 250 V and 650 V. Here, a phenomenon occurs that a single roving of the CFRP woven fabric sticks into the glass fiber layers and reduce the insulation distance.

According to equation (1), the dielectric strength of the glass fiber fabric with the corresponding matrix is more than 3.2 kV / mm.

Although the breakdown voltage could not be accurately specified, it has been shown that there is a risk of short which must be excluded during production. For this, at least two layers of GFRP must be used to create a working insulation.

Figure 5: Examination of the dielectric strength in the vertical and horizontal direction

In contrast to the previous scenario, the conductor tracks are arranged side by side in order to identify the required distance from one another. With this arrangement of the electrodes, the spacing of the conductor tracks can be set more individually. This, in turn, also leads to an increase in the manufacturing effort, since the conductor paths are precisely cut and aligned with each other by means of a measuring instrument. Figure 5 visualizes the difference in a sketch.

The distances between the electrodes were increased in steps of five tenths of a millimeter and were tested after consolidation. The results are shown in Figure 6. The values for CFRP electrodes are shown in blue and and the values for electrodes made of steel are displayed in red. For carbon fiber electrodes, a voltage can be applied only at a distance of 0.2 mm. At small distances little rovings and fiber filaments again lead to a short circuit. Similar to the electrodes arranged vertically above each other (Figure 4) the voltage can only be applied to a part of the samples, while other samples exhibit a short-circuit fault. Safe insulation up to 6.5 kV takes place at a distance of 0.5 mm.

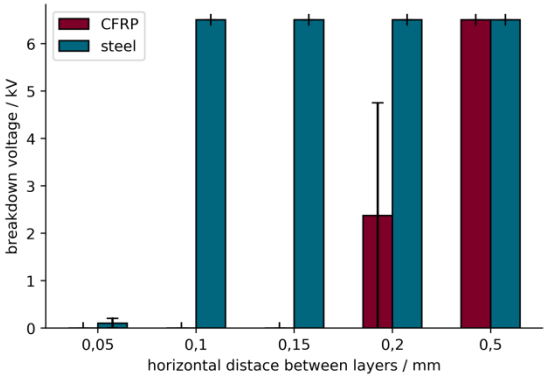

Figure 6: Breakdown voltage as a function of the horizontal distance

The steel foils are safely insulated above a distance of 0.1 mm. According to (1), the breakdown strength of the pure epoxy matrix is thus more than 6,5 kV / mm.

The results show that the steel foils can be characterized very well, the influences of the CFRP electrodes have to be examined more detailed.

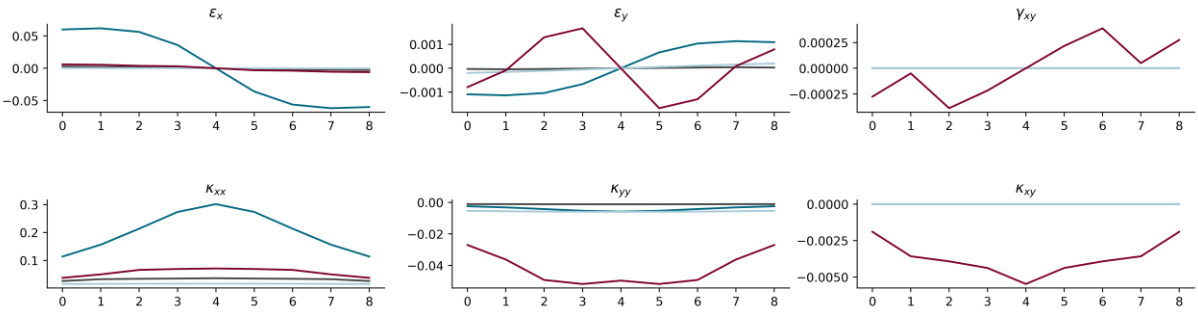

Figure 8: structural responses of the laminates to a bending load

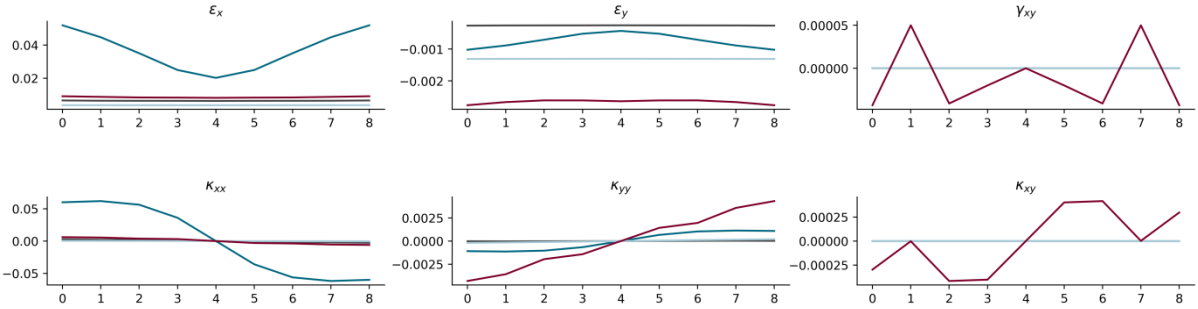

Figure 9: structural responses of the laminates to a tensile load

Positioning of the conductor track

Figure 7 shows the deflection of four eight-layer laminates subjected to a bending load. One metal foil was added to each laminate. For each calculation, the position of the metal foil travels one layer further through the laminate. The first position of the metal layer is on the outside of the laminate (position 0). A total of nine computation results are achieved for each laminate. The values were calculated using the classical laminate theory (CLT).

A carbon fiber of type M21/T700GC with a stiffness of 154,000 N / mm² and a steel foil with a strength of 200,000N / mm² were chosen as the calculation basis. The following four stackings were used:

$[90°_4]_S$, $[90°; 0°_2; 90°]_S$, $[0°_4]_S$,
$[45°; -45°; 0°; 90°]_S$

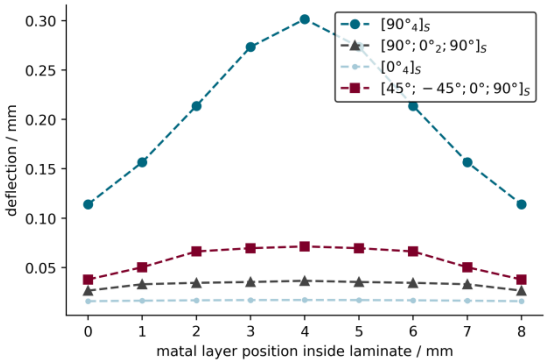

Figure 7: Deflection of the laminate as a function of the metal foil position

The figure shows how the metal foil affects the overall laminate behavior. For the $[90°_4]_S$ stack, the steel layers in the outer areas have the greatest influence in avoiding any deflection because of their distance to the neutral fiber.

The stiffer the laminate, the less is the influence of the metal foil. Since only symmetrical laminates were used for the calculation, the course of the deflection is also symmetrical to the central axis of the laminate.

Figure 8 shows all the elongations and distortions of the four laminates presented in the case of bending stress (calculated with CLT).

Especially for the already mentioned stack of 90° layers, the steel layers in the outer areas ensure an increased expansion (ϵ_x) on the opposite side. (blue line). The fourth stacking (red line) with the +/- 45° layers has a bending-drill coupling due to its construction [18]. The steel foil ensures a reduction of the deflection for the curvatures and for the twists. The asymmetry, in turn, provides a deformation in x and y directions (ϵ_x, ϵ_y).

The structural responses of the laminates to a tensile load are shown in Figure 9. It can be seen that the previously symmetrical layer stacking become unsymmetrical, and thus, bending-torsion and bending-elongation couplings are introduced into the laminate. In the design, the steel layers should be placed symmetrically into the laminate in order to prevent this effect.

Scaled Demonstrator

In order to be able to analyze and assess the potential of fiber reinforced composite with regard to structure-integrated conductor paths, a suitable demonstrator for the integration of the conductor was developed and built.

The demonstrator should show that it is possible to contact several components and

control units. For this purpose a voltage supply and a data communication integrated in the CFRP structure are necessary.
This Demonstrator contains the four required foil conductors: the 12 V supply voltage, the two CAN-Bus channels and the ground. It is contacted at suitable points in order to connect the various consumers as well as control units independently.
Fig. 10 shows the schematic structure with its layered structure. The individual layers are shown in the figure.

Figure 10: The sectional view of the demonstrator consisting of CFRP cover layers, GFRP insulation and conductive metallic intermediate layers

The demonstrator with the structure-integrated load carrying conductor tracks consists of the CFRP cover layers as well as the alternately layered GFRP insulation (two layers) and the conductive metallic intermediate layers. The metal layers represent the global cable harness. The inner layers of the harness are voltage supply, the outer layers the BUS architecture. (see Figure 10) Any module can be connected to this wiring harness.
The scale is chosen in such a way that the resulting dimensions of approx. 660 mm x 270 mm represent a good compromise between the handling and the demonstrability of the structure-integrated conductor tracks.
The two top layers (top / bottom) consist of a 1.6 mm quasi-isotropic CFRP structure. The middle section consists of an alternating structure of glass fiber and steel layers. The steel foils are blasted directly in front of the deposit in a special developed blasting system and treated with sol-gel to ensure good interlaminar strength (see [19]). The micro section of the structure is shown in Figure 11.

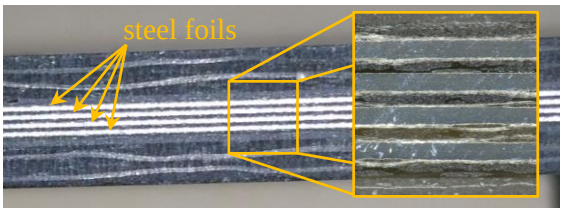

Figure 11: micro section of the demonstrator structure

During the investigation of the demonstrator, no errors could be detected in data communication or in the power supply. All connected components have been supplied with power and have received or sent commands via the CAN-Bus.

Conclusion

The integration of the conductor tracks significantly reduces or eliminates the manufacturing and assembly costs for the cable harness. The conductor tracks are integrated directly into the supporting structure and are thus able to realize both, the load transmission and the electrical signals transmission without any loss.
The transmission of the electrical signals works without any loss of functionality.
The conductor tracks thus make an important contribution to lightweight construction, weight reduction and resource conservation.

References

[1] Pat Wheeler. Technology for the More and All Electric Aircraft of the Future 2016.
[2] Pat Wheeler. Microsoft PowerPoint - EPE 2011 Keynote on MEA [Compatibility Mode].
[3] Xavier Roboam. New trends and challenges of electrical networks embedded in “more electrical aircraft” 2011.
[4] QI H, FU Y, QI X, LANG Y. Architecture Optimization of More Electric Aircraft Actuation System. Chinese Journal of Aeronautics 2011;24(4):506–13.

[5] Gohardani AS, Doulgeris G, Singh R. Challenges of future aircraft propulsion: A review of distributed propulsion technology and its potential application for the all electric commercial aircraft. Progress in Aerospace Sciences 2011;47(5):369–91.

[6] Kim H, Park M, Hsieh K. Fatigue fracture of embedded copper conductors in multifunctional composite structures. Composites Science and Technology 2006;66(7-8):1010–21.

[7] Kim HS, Kang JS, Park JS, Hahn HT, Jung HC, Joung JW. Inkjet printed electronics for multifunctional composite structure. Composites Science and Technology 2009;69(7-8):1256–64.

[8] W. Hufenbach. Integration and evaluation of mechanical and electrical joints in functionintegrative textile reinforced thermoplastic composites: ECCM15 - 15th European Conference on Composite Materials. Venice; 2012.

[9] J. Schmidt. Entwicklung eines Interfacekonzepts für integrierte Funktionselemente in UAV-Strukturen. Diplomarbeit. Technische Universität Braunschweig; 2011.

[10] Rehbein J, Wierach P, Gries T, Wiedemann M. Improved electrical conductivity of NCF-reinforced CFRP for higher damage resistance to lightning strike. Composites Part A: Applied Science and Manufacturing 2017;100:352–60.

[11] Chen Q, Guan Z, Li Z, Ji Z, Zhuo Y. Experimental investigation on impact performances of GLARE laminates. Chinese Journal of Aeronautics 2015;28(6):1784–92.

[12] B. Kolesnikov. Composite Material with a Reinforced Connecting Area(Patent PCT/DE99/00790).

[13] E. Petersen E, D. Stefaniak, C. Hühne. Efficient joint design using metal hybridization in fiber reinforced plastics. Stade; 2014.

[14] D. Stefaniak. Improving The Mechanical Performance Of Unidirectional CFRP by Metal-Hybridization: ECCM15 - 15th European Conference on Composite Materials. Venice; 24-28th 2012.

[15] Eksi S, Genel K. Bending response of hybrid composite tubular beams. Thin-Walled Structures 2013;73:329–36.

[16] Haedir J, Zhao X, Bambach MR, Grzebieta RH. Analysis of CFRP externally-reinforced steel CHS tubular beams. Composite Structures 2010;92(12):2992–3001.

[17] K.-H. Grote, J. Feldhusen (eds.). Dubbel: Taschenbuch für den Maschinenbau. 23rd ed. Berlin; 2011.

[18] C. Mittelstedt, W. Becker. Strukturmechanik ebener Laminate. 1st ed. Darmstadt; 2017.

[19] D. Stefaniak. Improving residual strength of unidirectionally reinforced plastic laminates by metal layering. Dissertation. Technische Universität Braunschweig; 2017.